

# Sensor-based Planning for Planar Multi-Convex Rigid Bodies

Ji Yeong Lee and Howie Choset

*Department of Mechanical Engineering*

*Carnegie Mellon University*

*5000 Forbes Avenue, Pittsburgh, PA15213, USA*

*jiyeongl@andrew.cmu.edu, choset@cs.cmu.edu*

**Abstract**—This paper presents a method for a planar rigid body consisting of multiple convex bodies to explore an unknown planar workspace, i.e., an unknown configuration space diffeomorphic to  $SE(2)$ . This method is based on a roadmap termed *concave hierarchical generalized Voronoi graph (concave-HGVG)*. Just as in our previous work, we decompose the free configuration space into contractible cells in which we define the *concave generalized Voronoi graphs (concave-GVG)*, and then connect these graphs using an additional structure termed *one-tangent edges*. Since the robot consists of multiple convex bodies, the *one-tangent edges* are defined using the diameter function of the convex hull of the convex bodies as well as the individual convex bodies. These two structures together form the *concave-HGVG*, which is a one-dimensional roadmap of the multi-convex bodies in plane. Both components are defined in terms of workspace distance measurement, and thus the *concave-HGVG* can readily be constructed in a sensor-based way.

## I. INTRODUCTION

This work considers sensor-based planning for a robot operating in a non-Euclidean configuration space. It is a step towards the ultimate goal of sensor-based planning for highly articulated bodies. Previously, the authors considered the planning problem for the point [5], [6] and rod-shaped robots operating in two- or three-dimensional workspaces [14], [8], as well as a convex body operating in a two-dimensional workspace [13]. As a next step, this work considers the planning for robot with a more general shape in a planar environment. More specifically, we consider a rigid planar body that can be represented as a union of a set of convex bodies, which we term *multi-convex rigid bodies*.

The main contribution of this work is a new roadmap termed *concave hierarchical generalized Voronoi graph (concave-HGVG)*. Recall that a *roadmap* is a one-dimensional structure in the configuration space which has the following three properties: accessibility, connectivity, and departability. A planner uses a roadmap to plan a path between two configurations in three steps: plan a path onto the roadmap (accessibility); plan a path along the roadmap (connectivity); and plan a path from the roadmap (departability) [2].

The configuration space for a rigid body operating in  $\mathbb{R}^2$  is three-dimensional and diffeomorphic to  $SE(2) \approx \mathbb{R}^2 \times S$ . Since it is not possible to define a one-dimensional deformation retract of the free configuration space with dimension three, we decompose the configuration space into contractible sets and, in each cell, define a retract termed *concave-GVG*

*edges*. Naturally, these retracts are not connected each other; to connect these retracts, we define another structure, termed *one-tangent edges*, which are defined using the geometry of each of the convex bodies or the union of two of convex bodies that comprise the multi-convex body. The union of the *concave-GVG edges* and the *one-tangent edges* form the *concave-HGVG*. Since both components of the *concave-HGVG* are defined using the workspace distance measurement, and equidistance relationship, the planner does not need to compute the decomposition explicitly, and can construct the *concave-HGVG* incrementally as it explores the space. The basic idea in defining these edges is that even if the robot consists of many convex bodies, to generate the path locally, the planner only need to consider the convex bodies that are close to the obstacles, just as the planner does not need to consider the obstacles that are far from the current robot configuration. Since these edges are defined in terms of the workspace distance measurement, the connectivity of the whole structure, i.e., the *concave-HGVG*, is guaranteed from the connectivity of the workspace.

The outline of the paper is as follows. In Section II, we review the prior work related to this paper. Section III defines the *concave-HGVG* and Section IV discusses the roadmap properties of the *concave-HGVG*. Finally, in Section V, we summarize the results and discuss the future directions.

## II. RELATED PRIOR WORK

This work is one step towards the ultimate goal of sensor-based planning for highly articulated bodies and one of the series of the roadmaps using the ideas based on the generalized Voronoi diagram (GVD). The GVD is defined as the set of points equidistant to two obstacles (Figure 1 (left)). Ó'Dúnlaing and Yap [17] first applied the GVD to the robot motion planning. They showed that the GVD is a deformation retract of the free space in  $\mathbb{R}^2$ , and thus has the property of the accessibility, connectivity and departability. In other words, the GVD is a roadmap for the point robot in the plane. They applied GVD to path planning for a disk-shaped robot operating in the plane, however, their result required the full knowledge of the workspace.

Choset and Burdick [4], [3] extended the GVD into three dimensions by defining the *generalized Voronoi graph (GVG)* which is the set of points equidistant to three obstacles. The

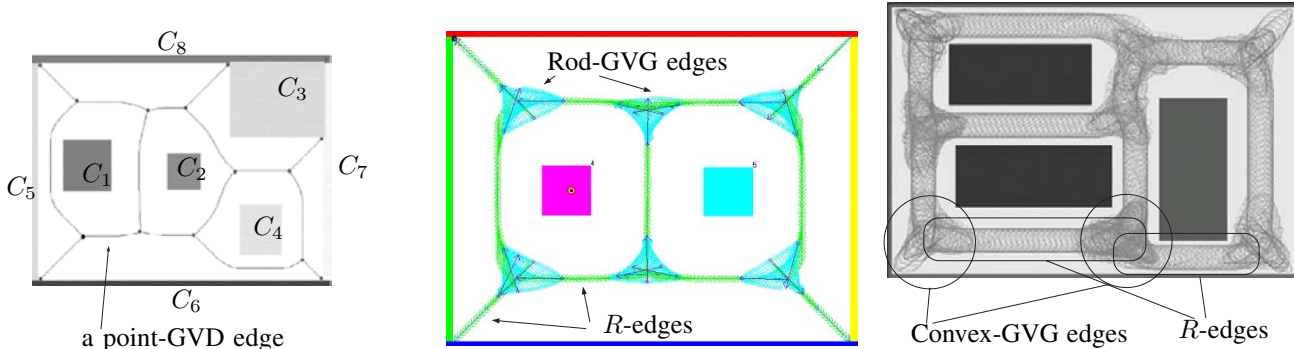


Fig. 1. (Left) Point-GVD in plane (Center) Rod-HGVG in plane (Right) Convex-HGVG in plane

GVG, by itself, is not connected in general and thus additional structures, called higher order GVG's were introduced, yielding a connected roadmap called the *hierarchical generalized Voronoi graph* (HGVG).

The next step in this line of research is to consider a rod-shaped robot. A rod is a line segment with a notion of direction. Early approaches [1], [9], [10], [16] which considered the rod or the polygonal/polyhedral bodies are, in general, restricted to the environments with polygonal or polyhedral obstacles and also require a full knowledge of the environment. Contrary to our method, most of the earlier works do not guarantee the connectivity of the roadmap since they employ some heuristics to connect the disconnected components.

Choset *et al.* [7], [8] defined a roadmap, termed the *rod hierarchical generalized Voronoi graph* (rod-HGVG, Figure 1 (center)), for rod-shaped robots operating in the plane. The authors extended this result for the convex body operating in the plane [13], resulting in the *convex hierarchical generalized Voronoi graph* (convex-HGVG) which is the basis of the current work (Figure 1 (right)) in this paper.

It is also worth noting that Lin *et al.* [11], [12], [18] and others developed the algorithms that combine generalized Voronoi graph with a probabilistic method to define a roadmap for the rigid bodies in two and three dimensional spaces.

### III. CONCAVE HIERARCHICAL VORONOI GRAPH DEFINITIONS

This work considers the concave bodies that can be represented as the union of a finite number convex bodies. Since the concave-HGVG is defined in terms of the workspace distance, it is necessary to consider the local geometry of the concave body, and thus it is reasonable to model the concave body as the union of the convex bodies. Moreover, this approach is a stepping stone for the planning of the snake robots, since the snake robots can be modelled as multiple convex links connected together.

#### A. Definitions

The rigid planar body is assumed to operate in a bounded planar environment, populated by obstacles. The configuration

space for the rigid planar body operating in a plane is three-dimensional, and diffeomorphic to  $SE(2)$ . We assume that the obstacles are a union of finite number of convex obstacles.

The robot is denoted as  $R$  and is represented as the union of the convex bodies  $R^a$  ( $a = 1, \dots, n$ )<sup>1</sup>. We assume that there is a series of range sensors along the boundary of the robot. Let  $q$  be the configuration of the robot, which can be parametrized as  $(x, y, \theta)$ . Let  $R(q)$  be the workspace volume occupied by the robot at the configuration  $q$ , and  $R^a(q)$  be the workspace volume occupied by the convex body  $R^a$  at the configuration  $q$ . Also, let  $C_i$  denote the workspace obstacles, and  $FCS$  be the free configuration space, i.e.,  $FCS = \{q \in SE(2) : R^a(q) \cap C_i = \emptyset \ \forall a \text{ and } i\}$ .

The distance between a convex body of the robot and an obstacle is defined as follows (Figure 2).

$$D_i^a(q) = \min_{x \in R^a(q), c \in C_i} \|x - c\|, \quad (1)$$

that is,  $D_i^a(q)$  is the *workspace distance* between the convex-body  $R^a$  and the obstacle  $C_i$ . Let  $r_i^a$  and  $c_i^a$  be the closest points on the convex-body  $R^a$  and the obstacle  $C_i$ , respectively. Note that we do *not* define the distance between the *whole concave body*  $R$  and a obstacle  $C_i$ .

The components of the concave-HGVG are defined using equidistance relationships based on the distance function defined above. The *two-equidistant surface* is defined as

*Definition 1 (Two-equidistant surface):*

$$CF_{ij}^{ab} = \{q \in FCS : 0 \leq D_i^a(q) = D_j^b(q) \leq D_k^c(q) \text{ for all } (k, c) \neq (i, a), (j, b), \text{ and } \nabla D_i^a(q) \neq \nabla D_j^b(q)\}, \quad (2)$$

where  $\nabla D_i^a(q)$  denotes the gradient of the distance function [13]. The condition  $\nabla D_i^a(q) \neq \nabla D_j^b(q)$  is required to guarantee that  $CF_{ij}^{ab}$  is indeed a two dimensional manifold.

We term  $(i, a) = (k, c)$  if and only if  $i = k$  and  $a = c$ . This means that there can be a two-equidistant face of the form  $CF_{ii}^{ab}$ , i.e., the robot is two-equidistant to a single obstacle  $C_i$ . Note that even when the two-equidistant surface is defined by one obstacle, it is still two-dimensional. Also note that if  $a = b$

<sup>1</sup>The indices  $i, j, k, \dots$  are used for the workspace obstacles, and the indices  $a, b, c, \dots$  are used for the convex bodies consisting the robot

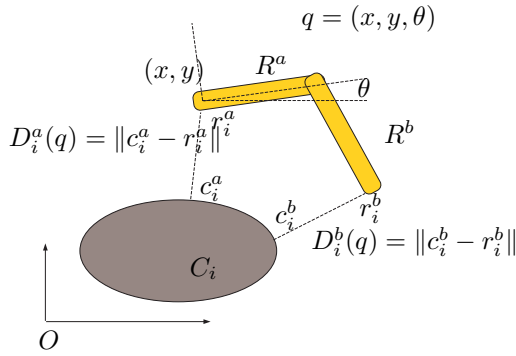


Fig. 2. The robot configuration and the distance function. The robot configuration  $q$  can be parameterized by  $(x, y, \theta)$ . The distance  $D_i^a$  between the convex body  $R^a$  and the convex obstacle  $C_i$  is defined as the minimum distance between two sets  $R^a$  and  $C_i$ . The distance  $D_i^b$  between the convex body  $R^b$  and  $C_i$  is similarly defined. Note that if  $D_i^a$  and  $D_i^b$  have same values, then the configuration  $q$  is defined to be double equidistant to the obstacle  $C_i$ .

for  $CF_{ij}^{ab}$ , then this means that the one of the convex bodies in the robot is closer to the two obstacles than any other convex bodies in the robot.

### B. GVG Edges

Since the planar body has three degrees of freedom, the *concave-GVG edge* is naturally defined with three-equidistant configurations. In other words, the concave-GVG edge can be defined as the intersection of the two-equidistant surface.

*Definition 2 (Concave-GVG edges):*

$$CF_{ijk}^{abc} = CF_{ij}^{ab} \cap CF_{jk}^{bc} \cap CF_{ik}^{ac}. \quad (3)$$

See Figure 10.1 for an example of the concave-GVG edges. It is possible that we have  $a = b$  or  $b = c$ , or even  $a = b = c$ . If  $a = b = c$ , this means that along the convex-GVG edge, one of the convex bodies is closest to the three obstacles. Such an edge looks like a GVG edge for a single convex body robot[13]. Also, it is possible that  $i = j$ , or  $i = k$ ; that is, the robot can be three-way equidistant to two obstacles. As we can see in Figure 3, it is necessary to trace the concave-GVG edges defined by less than three obstacles, to guarantee the connectivity of the concave-HGVG.

Actually, the robot cannot determine the number of the convex workspace obstacles that it is closest to. The robot determines that it is three-way equidistant by comparing the values of the sensor reading along the boundary of the robot. The number of the local minima determines the number of the obstacles that the robot “sees”, and three of the local minima has same value, and the robot decides that it is three-way equidistant to the three obstacles. However, we assume that it is not possible to have the concave-GVG edges formed by one obstacle, that is, it is not possible to have the concave-GVG edge of the form  $CF_{iii}^{abc}$ , since it could result in a two dimensional structure (Figure 4). With this assumption, the concave-GVG edge is in general one-dimensional.

The concave-GVG edges can intersect each other, forming the *meet configurations*. That is, a meet configuration is a four-

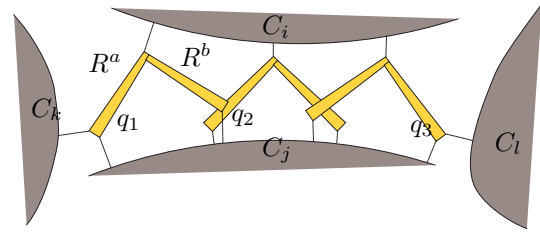


Fig. 3. The L-shaped robot travels between the two parallel walls. All configurations shown in the figure belong to the two-equidistant face  $CF_{ijj}^{abb}$ . The configuration  $q_1$  lies on the intersection of the GVG edges  $CF_{ijk}^{aaa}$  and  $CF_{ijl}^{aab}$ , and the configuration  $q_3$  lies on the intersection of the GVG edges  $CF_{ijj}^{abb}$  and  $CF_{ijl}^{aab}$ . That is, the two GVG edges  $CF_{ijk}^{aaa}$  and  $CF_{ijl}^{aab}$  are connected by another GVG edge  $CF_{ijj}^{abb}$ . It is easy to see that there is no one-tangent connecting  $CF_{ijk}^{aaa}$  and  $CF_{ijl}^{aab}$ .

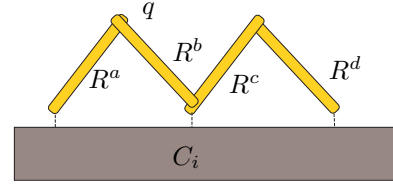


Fig. 4. The robot consists of four convex bodies. The configuration  $q$  lies on the GVG edge  $CF_{iii}^{abd}$ , and from the configuration  $q$ , and any translational motion would leave the robot on the GVG edge  $CF_{iii}^{abd}$ . That is the GVG edge  $CF_{iii}^{abd}$  is two dimensional.

way equidistant configuration. Again, the meet configuration can be formed by less than four obstacles.

Since the concave-GVG edge is defined in terms of workspace distance measurement, it can be readily constructed in a sensor-based way, using a curve tracing method described in [6]. The robot terminates tracing a concave-GVG edge if it reaches a meet configuration or a boundary configuration (i.e., a configuration where the distance to the closest obstacles are zero). When the robot reaches a meet configuration, it chooses an untraced concave-GVG edge and begins tracing it. If all edges are traced or the robot reaches a boundary configuration, it returns to a next meet configuration with unexplored edges, and traces them.

### C. One-tangent Edges

As in the planar rod-HGVG and the convex-HGVG, the concave-GVG is not connected in general in a connected free configuration space. To connect the disconnected concave-GVG edges, we use the two-equidistant structure, termed *one-tangent edges*.

Recall that the set of the two equidistant configuration is two-dimensional, and thus, to form a one-dimensional structure, we need an additional constraint. To provide the additional constraint, we use the *diameter function* (or radius function [15]) and the *principal axes*.

First, we discuss the diameter function and the principal axis for a convex body  $R$ . Let  $N$  be the unit vector in a reference direction and  $\theta$  be the orientation of the body  $R$  with respect to  $N$ . Then, the value of diameter function  $h : S^1 \rightarrow \mathbb{R}$  is

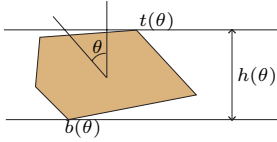


Fig. 5. Diameter function  $h(\theta)$ . The top (point  $t$ ) and bottom (point  $b$ ) determine the value of  $h(\theta)$ .

defined to be  $\max_{t,b \in R(\theta)} (t - b) \cdot N$ , where  $R(\theta)$  is the set of the points occupied by a convex set  $R$  oriented at  $\theta$ . We call the two points  $t$  and  $b$  that determines the value of  $h(\theta)$  at given orientation as *top* and *bottom* points (Figure 5).

Then, we use the local minima of the diameter function to define the principal axes. Let  $t : S^1 \rightarrow \mathbb{R}^2$  and  $b : S^1 \rightarrow \mathbb{R}^2$  the top and bottom points on a the body in a body-fixed coordinate frame for a given orientation. Let  $\{\theta_i^*\}$  be the set orientations where the diameter function  $h$  obtains minimal values. A *principal axis*  $v_i$  is the unit vector that is normal to the vector  $(t(\theta_i^*) - b(\theta_i^*))$ .

For the concave body, the diameter function and the principal axis can be similarly defined, except that for a given principal axis, the points  $t$  and  $b$  may not be uniquely defined. Actually, it is not difficult to see that the value of the diameter function is the same for a concave body and the convex hull of the concave body.

Now, for the convex-HGVG, the one-tangent edge was defined using the principal axis so that the resulting one-tangent edge is a path between two three-way equidistant edges which maximizes the minimum distance along the path (see [13] for detail.) Naively we could define the principal axis using the diameter function of the whole concave body, or of the convex hull of the concave body (which is actually same). However, for the multi-convex bodies, this idea does not result in a correct definition of the one-tangent edges, as we can see from the examples in Figure 6 and Figure 7. From these examples, it is clear that, to define one-tangent edge for the multi-convex bodies, we need to consider the convex hull of the union of the convex bodies in the multi-convex body as well as the individual convex bodies.

Since we define the one-tangent edges as two-way equidistant paths, we only need to at most two convex bodies in defining the one-tangent edges. Thus, in defining one-tangent edges for the concave body, we only need to consider the diameter function of the union of two of convex bodies inside the concave body as well as the diameter function of each of the convex bodies.

Now we define the one-tangent formally. Let  $v_k^{ab}$  denote a principal axis, defined by the convex bodies  $R^a$  and  $R^b$ , where the index  $a$  and  $b$  could be the same. The index  $k$  is used since there can be multiple principal axes for a convex body or for the union of two convex bodies. Then, the definition of the one-tangent edge is essentially same as that of the convex one-tangent edge, i.e.,

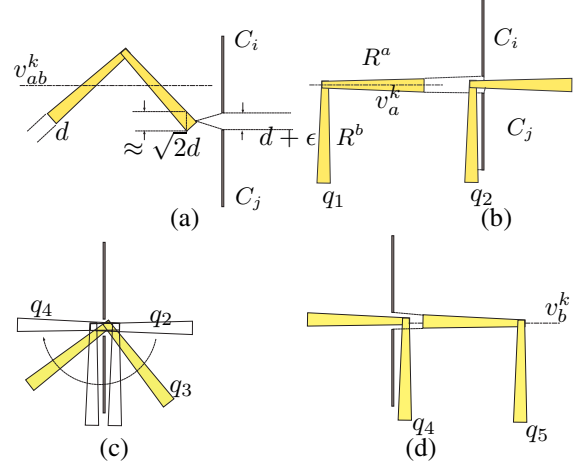


Fig. 6.  $L$ -shaped robot passing through a small gap. (a)  $L$ -shaped robot and two obstacles. The width of the convex bodies  $R^a$  and  $R^b$  at one end is  $\delta$  and the gap between  $C_i$  and  $C_j$  is  $\delta + \epsilon$  ( $\epsilon \approx 0$ ). Clearly the robot can pass through the gap between two obstacles even if the convex hull of the robot cannot. However, using the principal axis defined by the whole concave body, the robot cannot align itself correctly to pass through the gap. Instead, by using the principal axis defined by each body, the robot can travel from the one side to the other side: (b) The robot traces the two-equidistant path, aligning itself using the principal axis defined by the body  $R^a$ . (c) At the configuration  $q_2$ , the robot becomes three-way equidistant, that is  $D_i^a(q_2) = D_j^a(q_2) = D_j^b(q_2)$ . Thus, the robot traces the GVG edge  $CF_{ij}^{abb}$  to travel through  $(q_2, q_3, \text{ and } q_4)$ . At  $q_4$ , the robot begins to trace the two-equidistant path using the body  $R_b$ , to the configuration  $q_5$ . Note that the configurations  $q_2$  and  $q_4$  are not actually the end points of the GVG edge.

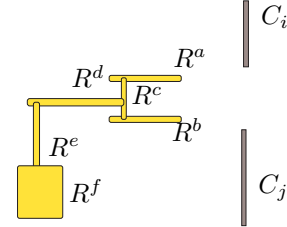


Fig. 7. The robot with six convex bodies. To enter the gap between the obstacles  $C_i$  and  $C_j$ , the robot first only needs to align itself using the principal axis defined by the bodies  $R^a$  and  $R^b$ , and trace the two-way equidistant path. To go through the gap, the robot needs to consider various combination of the convex bodies comprising the robot, but does not need to consider more than four of them at the same time. To exit from the gap, the robot only needs to use the body  $R_f$ , without considering the other convex bodies.

*Definition 3 (One-tangent edge):*

$$R_{ij}^{ab} = \{q \in CF_{ij}^{ab} \mid \langle c_i(q) - c_j(q), v_k^{ab} \rangle = 0 \text{ for some } k\}, \quad (4)$$

where  $c_i(q)$  and  $c_j(q)$  are the closest points on  $C_i$  and  $C_j$ , respectively, and  $\langle \cdot, \cdot \rangle$  denotes the inner product. See Figure 10.2 for an example of the one-tangent edges.

It turns out that we need another type of two-way equidistant edges. First consider the following example in Figure 8. For the robot to move from the configuration  $q$  to the configuration  $q'$ , it must trace a two-way equidistant path defined by the obstacle  $C_6$  and the convex bodies  $R^b$  and  $R^c$ . However, according to the definition of the one-tangent edge given above, there is no one-tangent that makes this motion possible.

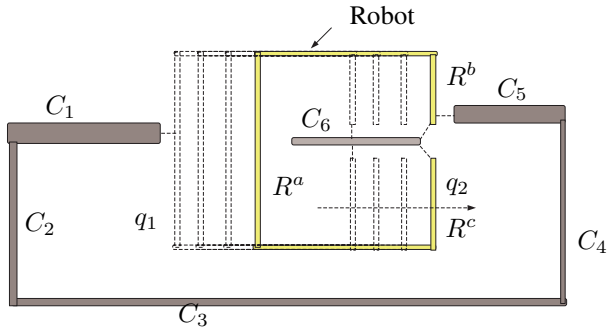


Fig. 8. The robot consists of five convex bodies (only relevant ones are labelled). For the robot to move from the configuration  $q_1 (\in CF_{166}^{abc})$  to  $q_2 (\in CF_{566}^{bbc})$ , the robot need to trace a two-way equidistant path (drawn in dotted lines) defined by the obstacle  $C_6$  and the convex bodies  $R^b$  and  $R^c$ . However, the principal axis defined by the body  $R^b$  and  $R^c$  is, in the figure, is vertical direction, and thus, the robot cannot orient itself correctly using the principal axis to make the motion.

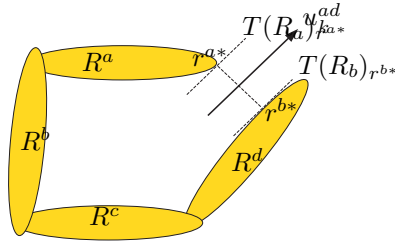


Fig. 9. The gap axis  $u_k^{ad}$  is defined by the convex bodies  $R_a$  and  $R_d$ . The points  $r^{a*}$  and  $r^{d*}$  are the closest point on the convex bodies. The gap axis  $u_k^{ad}$  is parallel to the tangents of  $R_a$  and  $R_d$  at  $r^{a*}$  and  $r^{d*}$ , respectively.

The problem here is, to make the desired motion possible, the planner need to plan a path as if the obstacle  $C_6$  is passing through the convex bodies  $R^a$  and  $R^e$ ; that is, the planner need to consider the convex obstacle as the robot, and the convex bodies of the robot as the convex obstacles. This would be possible if the planner has the prior information of the obstacles, which is not the case in this work. That is, the planner cannot have the principal axes of the obstacles prior to exploration.

To fix this situation, we introduce another type of one-tangent edge, which is a slight modification of the one-tangent edge given above. First, instead of the principal axis defined using the obstacle geometry, we introduce the *gap axis*, defined by the convex bodies of the robot. Let  $R^a$  and  $R^b$  be the two convex bodies, whose relative position is fixed. Let  $r^{a*}$  and  $r^{b*}$  be the closest points on  $R^a$  and  $R^b$  between them. Then, the *gap axis*  $u_k^{ab}$  is defined as the vector normal to the line segment connecting  $r^{a*}$  and  $r^{b*}$  (Figure 9).

Then the *dual one-tangent* edge using this gap axis  $u_k^{ab}$  is defined as

**Definition 4 (Dual one-tangent edges):**

$$Z_{ij}^{ab} = \{q \in CF_{ij}^{ab} : \langle u_k^{ab}, r_i - r_j \rangle = 0\}. \quad (5)$$

As the name suggests, the dual one-tangent edge  $Z_{ij}^{ab}$  can be thought as a dual of the one-tangent edge  $R_{ij}^{ab}$ . Because of the way it is defined, it can be shown that if, between two

GVG-edges, there is a two-way equidistant path so that the obstacle passes through the gap between the convex bodies, there must be a dual one-tangent edge  $Z_{ij}^{ab}$  that connect the two GVG-edges. Note that, for the dual one-tangent edge  $Z_{ij}^{ab}$ , the convex body  $R^a$  and  $R^b$  cannot be the same. However,  $C_i$  and  $C_j$  could be the same or be different from each other.

Since the point  $c_i$  can easily computed from the sensor reading, and  $v_k^{ab}$  is known from the geometry of the robot, the one-tangent edges can be readily constructed using only sensor information by the method described in [13]. While tracing a concave-GVG edge, the planner checks if the robot lies on the intersection of the concave-GVG edge and a one-tangent edge. Then, after tracing the current concave-GVG edge, the robot backtraces the concave-GVG edge to the point of intersection, and begins tracing the one-tangent edge. A one-tangent edge terminates on either a three-way equidistant configuration or a boundary configuration (i.e., a configuration where the distance to the two closest obstacles are zero). From the three-way equidistant configuration, which, by definition, on a GVG edge, the robot begin tracing the GVG-edge.

Then the concave-HGVG, denoted by  $G$  is defined as the union of the concave-GVG edges and the one-tangent edges, i.e.:

**Definition 5 (Concave-HGVG):**

$$G = (\cup CF_{ij}^{ab}) \cup (\cup R_{ij}^{ab}) \cup (\cup Z_{ij}^{ab}) \quad (6)$$

Figures 10, 11 show some examples of the concave-HGVG in simple environments.

#### IV. ROADMAP PROPERTIES OF THE CONCAVE-HGVG

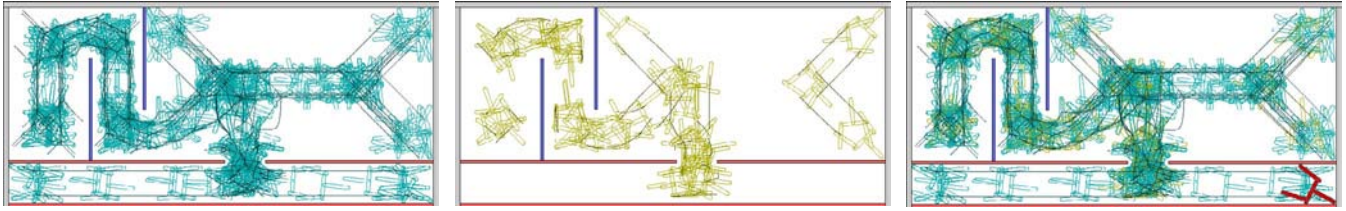
In this section, we show that the convex-HGVG defined in the previous section indeed satisfies the roadmap properties. Recall that the roadmap has three properties: accessibility, departibility and connectivity. The accessibility means that there is a path from an arbitrary configuration in the free configuration onto the concave-HGVG, and the departibility is the reverse of the accessibility. The connectivity means that if the free configuration space is connected, the concave-HGVG is connected also.

For the accessibility, we use a series of the fixed-orientation gradient ascent operations from the closest obstacles, as in the convex-HGVG [13]. It can be proven that after the gradient ascent operation, the robot reaches a three-way configuration, which is an element of a concave-GVG edge. This gradient ascent operation implicitly defines a function  $H$ . That is, for an arbitrary configuration  $q$ ,  $H(q) \in \cup CF_{ijk}^{abc}$ .

Also, as in convex-HGVG, we define the junction region  $J_{ijk}^{abc}$  as a pre-image of a concave-GVG edge  $CF_{ijk}^{abc}$  under the accessibility function. That is

$$J_{ijk}^{abc} = \{q \in FCS : H(q) \in CF_{ijk}^{abc}\}. \quad (7)$$

The junction regions define an exact cellular decomposition of the free configuration space, and since it can be shown that the accessibility function  $H$  is continuous in a connected component of a junction region, a concave-GVG edge is a deformation retract of a junction region. These retracts,

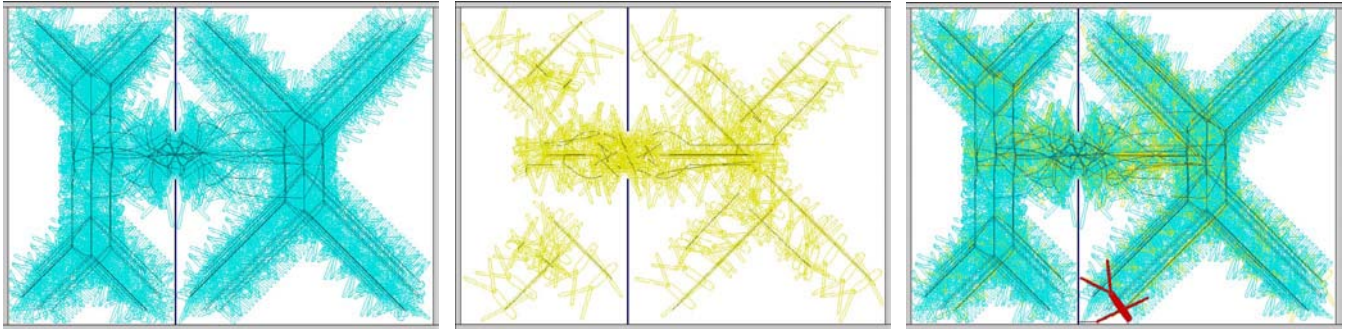


(1) GVG edges

(2) One-tangent edges

(3) Concave-HGVG

Fig. 10. The placements of the robot along the concave-HGVG. The robot consists of four convex bodies. The dark lines represent the trajectory of the reference point on the robot.



(1) GVG edges

(2) One-tangent edges

(3) Concave-HGVG

Fig. 11. The placements of the robot along the concave-HGVG. The robot consists of four convex bodies. The dark lines represent the trajectory of the reference point on the robot.

however, are not in general, connected to each other, and that is why we need the one-tangent edges. Our goal is to show that these retracts together with the one-tangent edges, i.e., the concave-HGVG forms a connected set.

First, we decompose the concave-HGVG in two parts, depending on how many concave bodies are closest to the obstacles on a given configuration on the concave-HGVG. More specifically, we decompose the concave-HGVG into the components where the closest convex body is unique and the components where there are more than one closest convex bodies.

We are going to use the structure of the convex-HGVG to understand the components of the concave-HGVG that has a unique closest obstacle. Note that if a configuration on the concave-HGVG has a unique closest convex body, then this is also an element of the convex-HGVG for the convex body. Thus, we first consider the convex-GVG edges for the individual convex bodies  $R^a$  of the concave body. Note that the free configuration space of  $R^a$  can also be parametrized by  $(x, y, \theta)$ . Moreover, without loss of generality, we can fix the reference point of  $R^a$  at the reference point of  $R$  (possibly lying outside of  $R^a$ ). Then clearly, if at a configuration  $q$ ,  $R^a(q)$  intersects an obstacle, then  $R(q)$  also intersects the obstacle. From this we can consider the free configuration space  $FCS$  of  $R$  as a subset of the free configuration space  $FCS^a$  of  $R^a$ . Then, it follows that the free configuration space is a subset of the union of  $FCS^a$ 's for all  $R^a$ . Recall that we are assuming the the free configuration space  $FCS$

is connected. Therefore, without loss of generality, we can assume each of  $FCS^a$  is connected also <sup>2</sup>.

First, let's fix some notations, and make some observations. Let  $G^a$  be the convex-HGVG of a given convex body  $R^a$ , and let  $GG^a$  and  $GR^a$  be the union of the GVG edges and the union of the one-tangent edges of the  $G^a$ , respectively. Also let  $G_v^a$  be the set  $G^a \cap FCS$ , i.e., the portions of the convex-HGVG defined by  $R^a$ , lying in the free configuration space of the concave body. Finally, let  $GG_v^a$  and  $GR_v^a$  be the GVG edges and the one-tangent edges of  $G_v^a$ . Then the concave-HGVG is represented as  $G = G_m \cup (\cup_a G_v^a)$ , where  $G_m = G - (\cup_a G_v^a)$ . That is, the set  $G_m$  is the set of the concave-HGVG edges that are defined by more than one convex body. Also, let  $GG_m$  and  $GR_m$  be the concave-GVG edges and the one-tangent edges of the  $G_m$ . Note that, by assumption,  $G^a$  is connected. However, the set  $G_v^a = G^a \cap FCS$  may not be connected.

We consider the boundary components of  $GG_v^a$  and  $GR_v^a$ . The boundary components of  $GG_v^a$  contain the boundary configurations (where the distance to the closest obstacle is zero) and the configurations where more than one convex bodies are closest to the obstacles. This means that the  $GG_v^a$  is connected to the components of the set  $G_m$ . This configuration is, by definition, a meet configuration, defined by more than one convex body. The boundary components of  $GR_v^a$  contain

<sup>2</sup>Actually,  $FCS^a$  could be disconnected even if  $FCS$  were connected. However, in that case, we could just consider the connected component of  $FCS^a$  that contains the  $FCS$ .

the boundary configurations, and the three-way equidistant configurations defined by either one convex body (i.e., the configurations lying on  $GG^a$ ) or two convex bodies (i.e., the configurations lying on  $GG_m$ ). As before, this means that the  $GR_v^a$  is connected to the components of the set  $G_m$ . Note that neither  $GG_v^a$  nor  $GR_v^a$  intersects the set  $GR_m^a$ , i.e., the one-tangent edges defined by two convex bodies.

Now, to show the connectivity, we need to show that if there is a path between the two arbitrary configurations  $q_1$  and  $q_2$  in the free configuration space, there is also a path between these two configurations along the concave-HGVG. From the accessibility, we can assume the configurations  $q_1$  and  $q_2$  lie on the concave-GVG edges. Moreover we can assume that the junction regions of these concave-GVG edges are adjacent, i.e., share a common boundary, and show that there is a path  $p_{ij}(t)$  along the concave-HGVG between  $q_1$  and  $q_2$ . If these two junction regions are not adjacent, then to find a path between them, we can just concatenate the paths  $p_{ij}(t)$ 's between the adjacent junction regions together with the GVG-edges, which, by definition, is a connected set in a connected components of the junction region. Thus, from now on, we consider only adjacent junction regions, and drop the indices for the path  $p(t)$ .

Let  $J_{(i)}$ <sup>3</sup> and  $J_{(j)}$  be two adjacent junction regions, i.e.,  $J_{(i)}$  and  $J_{(j)}$  share a common boundary. This means that there is a path between  $CF_{(i)}$  and  $CF_{(j)}$ . Then, as in [13], by applying gradient ascent from the closest obstacle, a two-way equidistant path  $p(t)$  ( $t \in [0, 1]$ ) can be obtained. Thus, we can assume that if two junctions are adjacent to each other, there is a two-way equidistant path between the retracts, i.e., the concave-GVG edges, of the junction regions.

Thus our goal is to show that, if there is a two-way equidistant path between two concave-GVG edges, they also are connected by a components of the convex-HGVG.

We consider three different cases depending on the number of the closest obstacles and the number of the closest convex bodies along the path  $p(t)$ . Note that the number of the closest obstacles can be assume to be constant along the path  $p(t)$ . Otherwise, it implies that there is a three-way equidistant configuration  $q$  on the path  $p(t)$ , and then we can consider the two paths from  $p(0)$  to  $q$  and  $q$  to  $p(1)$ .

Now, the path  $p(t)$  can be formed between (i) two obstacles and one convex body (i.e.,  $p(t)$  lies on  $CF_{ij}^{aa}$ ) (ii) two obstacles and two convex bodies ( $p(t)$  lies on  $CF_{ij}^{ab}$ ), or (iii) one obstacle and two convex bodies ( $p(t)$  lies on  $CF_{ii}^{ab}$ ).

For case (i), where the path  $p(t)$  is defined by one convex body, and following a result from the convex-HGVG, there must be a one-tangent edge connecting two convex-GVG edges, defined by the convex body. Now, these two convex-GVG edges are the elements of  $GG^a$ , and may not entirely lie in the concave-HGVG, and the point of intersection between the convex-GVG edges and the one-tangent edge found above may not lie in the concave-HGVG either. However, if this is the case, this just implies that the one-tangent edge intersects

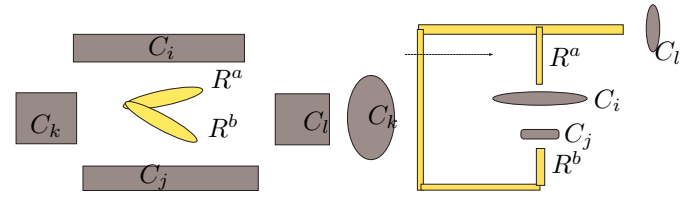


Fig. 12. The robot travels from the concave-GVG edge defined by obstacles  $C_i$ ,  $C_j$  and  $C_k$  and convex to the concave-GVG edge defined by  $C_i$ ,  $C_j$  and  $C_l$ , along the two-way equidistant path on  $CF_{ij}^{ab}$ . (Left) The robot moves between two obstacles. (Right) The two convex bodies of the robot envelope the closest obstacles as it travels on a two-way equidistant path.

some concave-GVG edge defined by the two closest obstacles and the convex body defining the  $p(t)$ , together with some other obstacle or other convex-body, which is connected to the convex-GVG edges.

For the case (ii), there are three subcases: (ii(a)) the convex hull of  $R^a$  and  $R^b$  passes through the gap between the obstacles  $C_i$  and  $C_j$  along  $p(t)$  (Figure 12 (left)), (ii(b)) the convex bodies  $R^a$  and  $R^b$  envelope the obstacles  $C_i$  and  $C_j$ ; that is, the convex hull of  $C_i$  and  $C_j$  can be seen as passing through the gap between the convex bodies  $R^a$  and  $R^b$  along  $p(t)$  (Figure 12 (right)), (ii(c)) other cases, that is, the convex bodies  $R^a$  and  $R^b$  “pass over” the obstacles  $C_i$  and  $C_j$  (Figure 13). These notion can be defined more formally as follows. First we define some notations. Let  $c_i^*$  and  $c_j^*$  be the closest points on  $C_i$  and  $C_j$  respectively, between  $C_i$  and  $C_j$ . Likewise  $r^{a*}(q)$  and  $r^{b*}(q)$  be the closest points between  $R^a$  and  $R^b$  on them, when the robot is at configuration  $q$ <sup>4</sup>. Then we can say the convex hull  $C_{ij}$  of  $C_i$  and  $C_j$  passes through  $R^a$  and  $R^b$ , if for all point  $x$  in  $C_{ij}$ , there is  $t \in [0, 1]$  so that the point  $x$  lies on the line segment connecting  $r^{a*}(p(t))$  and  $r^{b*}(p(t))$ , and  $C_{ij}$  “lies on the opposite sides”<sup>5</sup> of the line connecting  $r^{a*}(p(t))$  and  $r^{b*}(p(t))$  at  $t = 0$  and  $t = 1$ . The case (ii(b)) can be defined similarly. Then for the case (ii(a)), we can simply consider the convex hull of  $R^a$  and  $R^b$ , and can find a one-tangent edge define by the convex hull of  $R^a$  and  $R^b$ , and the obstacles  $C_i$  and  $C_j$ . For the case (ii(b)), we can find a dual one-tangent edge  $Z_{ij}^{ab}$  by considering the convex hull of the obstacles  $C_i$  and  $C_j$ . For case (ii(c)), we can actually find a three-way equidistant path by applying the gradient ascent to the path  $p(t)$ . That is, the two concave-GVG edges are connected by another concave-GVG edge.

Finally, for the case (iii), there are two subcases: (iii(a)) the obstacle “passes through the gap between ”  $R^a$  and  $R^b$  (Figure 14 (left)), and (iii(b)) the obstacle passes over the convex bodies  $R^a$  and  $R^b$  (Figure 14 (right)). Then the case (iii(a)) is essentially identical to the case (ii(b)), and the case (iii(b)) is essentially identical to the case (ii(c)).

Thus, we can conclude that if there is a path between the two concave-GVG edges, they are connected either by a one-

<sup>4</sup>Note that these points are fixed on the convex bodies, but can move relative to the world coordinate as the robot moves.

<sup>5</sup>Imagine as if the convex obstacles have been moved relative to the fixed robot.

<sup>3</sup>The subscript  $(i)$  represents a three-index set, for example  $J_{(i)} = J_{kjl}^{abc}$ .

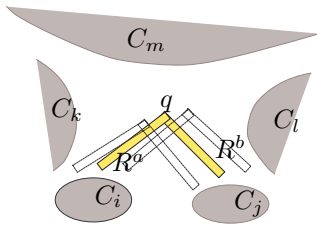


Fig. 13. The robot travels from the concave-GVG edge defined by obstacles  $C_i$ ,  $C_j$  and  $C_k$  and convex to the concave-GVG edge defined by  $C_i$ ,  $C_j$  and  $C_l$ , along the two-way equidistant path on  $CF_{ij}^{ab}$ . The two convex bodies moves “over” the two closest obstacles  $C_i$  and  $C_j$  between two concave-GVG edges (the configurations on the concave-GVG edges are denoted in dotted lines). This path can be deformed on to the concave-GVG edge  $CF_{ijm}^{aab}$ , so that this concave-GVG edge connects two concave-GVG edges.

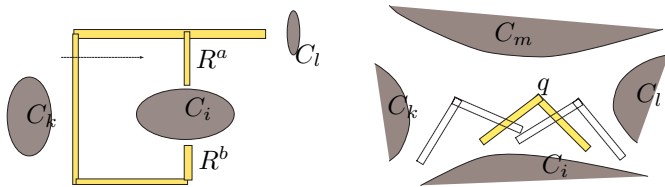


Fig. 14. (Left) The obstacle  $C_i$  is between two convex bodies  $R^a$  and  $R^b$ . (Right) The robot  $q$  is over the obstacle  $C_i$

tangent edge or another concave-GVG edge. Then, from this, we can conclude that the concave-HGVG is connected.

## V. CONCLUSION

This paper introduces a roadmap termed the *concave hierarchical generalized Voronoi graph* for the multi-convex rigid bodies operating in plane. The concave-HGVG is defined in terms of the workspace distance measurement, and thus can be constructed using only sensor information without prior knowledge of environment. The concave-HGVG comprises two components: (i) the concave-GVG edges, which are three-way equidistant structures and (ii) the one-tangent edges, which are two-way equidistant structure with additional constraint. In defining the one-tangent edges, we borrowed the ideas from the convex-HGVG and extended it for the multi-convex bodies. Since for the multi-convex bodies, the robot could be double equidistant from a single convex obstacle, in addition to the generalization of the one-tangent edges, we introduced another definition of the one-tangent edge, termed dual one-tangent edges.

Like the authors’ previous roadmap works, the definition of the concave-HGVG induces a decomposition of the free configuration space, in which the concave-GVG edges are the retracts of the cells, and the one-tangent edges connect the disconnected retracts.

The next step in this line of research is to extend the current work for *two-bodies*, operating in plane, that is, two convex bodies connected by a rotational joint that can have a joint limit. For the two-bodies, the concave-HGVG could be defined for each fixed-value of the internal joint angle. Specifically, some joint angles can be chosen so that the “workspace volume” is minimized in some measure. Then, the

concave-HGVGs for the concave bodies at those joint angles would form a backbone of the roadmap for the two-body, but naturally, those concave-HGVGs will not be connected together, and the major problem for two-body problem is to define new structures to connect those disconnected concave-HGVGs.

## REFERENCES

- [1] R. A. Brooks. Solving the Find-Path Problem by Good Representation of Free Space. In *IEEE Transaction on Systems, Man and Cybernetics*, volume SMC-13, No. 3, March/April 1983.
- [2] J.F. Canny. *The Complexity of Robot Motion Planning*. MIT Press, Cambridge, MA, 1988.
- [3] H. Choset and J. Burdick. Sensor Based Motion Planning: Incremental Construction of the Hierarchical Generalized Voronoi Graph. *International Journal of Robotics Research*, 19(2):126–148, February 2000.
- [4] H. Choset and J. Burdick. Sensor Based Motion Planning: The Hierarchical Generalized Voronoi Graph. *International Journal of Robotics Research*, 19(2):96–125, February 2000.
- [5] H. Choset and J.W. Burdick. Sensor Based Planning, Part i: The Generalized Voronoi Graph. In *Proc. IEEE Int. Conf. on Robotics and Automation*, Nagoya, Japan, 1995.
- [6] H. Choset and J.W. Burdick. Sensor Based Planning, Part ii: Incremental Construction of the Generalized Voronoi Graph. In *Proc. IEEE Int. Conf. on Robotics and Automation*, Nagoya, Japan, 1995.
- [7] H. Choset and J.W. Burdick. Sensor Based Planning for a Planar Rod Robot. In *Proc. IEEE Int. Conf. on Robotics and Automation*, 1996.
- [8] H. Choset and J. Y. Lee. Sensor-Based Construction of a Retract-Like Structure for a Planar Rod Robot. *IEEE Transaction of Robotics and Automation*, 17(4):435–449, August 2001.
- [9] J. Cox and C.K. Yap. On-line Motion Planning: Case of a Planar Rod. In *Annals of Mathematics and Artificial Intelligence*, volume 3, pages 1–20, 1991.
- [10] Abhi Dattasharma and S. Sathiya Keerthi. An augmented Voronoi roadmap for 3D translational motion planning for a convex polyhedron moving amidst convex polyhedral obstacles. *Theoretical Computer Science*, 140(2):205–230, April 1995.
- [11] M. Frosky, M. Garber, M. Lin, and D. Manocha. A Voronoi-based Hybrid Motion Planner. In *Proceedings of the IEEE International Conference on Robots and Systems*, 2001.
- [12] K. Hoff, T. Culver, J. Key, M. Lin, and D. Manocha. Interactive Motion Planning Using Hardware-accelerated Computation of Generalized Voronoi Diagrams. In *Proceedings of the IEEE International Conference on Robotics and Automation*, 2000.
- [13] J. Y. Lee and H. Choset. Sensor-Based Exploration for Convex-Bodies: A New Roadmap for a Convex-shaped Robot. In *Proceedings of IEEE International Conference on Robotics and Automation*, pages 1675–1682, May 2002.
- [14] J.Y. Lee, H. Choset, and Alfred A. Rizzi. Sensor Based Planning for Rod Shaped Robots in Three Dimensions: Piece-wise Retracts of  $\mathbb{R}^3 \times S^2$ . In *Proceedings of IEEE International Conference on Robotics and Automation*, pages 991–999, May 2001.
- [15] M. T. Mason. *Mechanics of Robotic Manipulation*. MIT Press, August 2001.
- [16] C. Ó’Dúnlain, M. Sharir, and C.K. Yap. Generalized Voronoi Diagrams for Moving a Ladder. I: Topological Analysis. *Communications on Pure and Applied Mathematics*, 39:423–483, 1986.
- [17] C. Ó’Dúnlain and C.K. Yap. A “Retraction” Method for Planning the Motion of a Disc. *Journal of Algorithms*, 6:104–111, 1985.
- [18] C. Pisula, K. Hoff, M. Lin, and D. Manocha. Randomized Path Planning for a Rigid Body Based on Hardware Accelerated Voronoi Sampling. In *Proc. Workshop on Algorithmic Foundations of Robotics*, 2000.